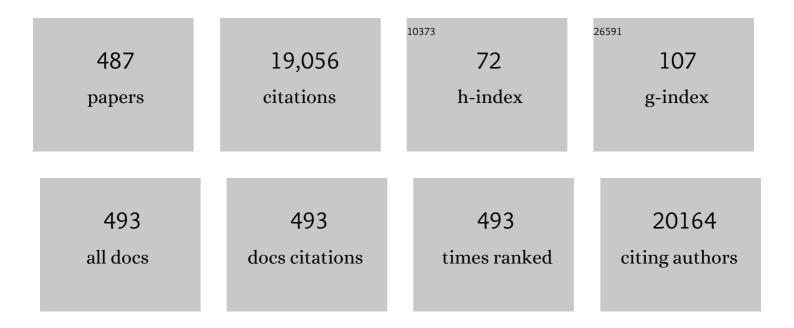
List of Publications by Year in descending order

Source: https://exaly.com/author-pdf/1291980/publications.pdf Version: 2024-02-01



#	ARTICLE	١٢	CITATIONS
1	Zinc Oxide Nanostructures for NO2 Gas–Sensor Applications: A Review. Nano-Micro Letters, 2015, 7, 97-120.	14.4	649
2	Zinc oxide nanonail based chemical sensor for hydrazine detection. Chemical Communications, 2008, , 166-168.	2.2	442
3	Biomass-derived nitrogen-doped carbon quantum dots: highly selective fluorescent probe for detecting Fe3+ ions and tetracyclines. Journal of Colloid and Interface Science, 2019, 539, 332-341.	5.0	424
4	Green synthesis of CuO nanoparticles with leaf extract of Calotropis gigantea and its dye-sensitized solar cells applications. Journal of Alloys and Compounds, 2015, 632, 321-325.	2.8	277
5	Perovskite Solar Cells: Influence of Hole Transporting Materials on Power Conversion Efficiency. ChemSusChem, 2016, 9, 10-27.	3.6	267
6	ZnO nanoparticles induced oxidative stress and apoptosis in HepG2 and MCF-7 cancer cells and their antibacterial activity. Colloids and Surfaces B: Biointerfaces, 2014, 117, 267-276.	2.5	254
7	Highly effective Fe-doped TiO 2 nanoparticles photocatalysts for visible-light driven photocatalytic degradation of toxic organic compounds. Journal of Colloid and Interface Science, 2015, 450, 213-223.	5.0	248
8	ZnO nanosheet networks and hexagonal nanodiscs grown on silicon substrate: growth mechanism and structural and optical properties. Nanotechnology, 2006, 17, 2174-2180.	1.3	212
9	Highly-sensitive cholesterol biosensor based on well-crystallized flower-shaped ZnO nanostructures. Talanta, 2009, 78, 284-289.	2.9	179
10	Influence of Sn doping on ZnO nanostructures from nanoparticles to spindle shape and their photoelectrochemical properties for dye sensitized solar cells. Chemical Engineering Journal, 2012, 187, 351-356.	6.6	176
11	Novel graphene/polyaniline nanocomposites and its photocatalytic activity toward the degradation of rose Bengal dye. Chemical Engineering Journal, 2012, 210, 220-228.	6.6	164
12	Comprehensive investigation of CO2 adsorption on Mg–Al–CO3 LDH-derived mixed metal oxides. Journal of Materials Chemistry A, 2013, 1, 12782.	5.2	164
13	Chemical Sensing Applications of ZnO Nanomaterials. Materials, 2018, 11, 287.	1.3	160
14	ZnO nano-mushrooms for photocatalytic degradation of methyl orange. Materials Letters, 2013, 97, 100-103.	1.3	156
15	Ce-doped ZnO nanoparticles for efficient photocatalytic degradation of direct red-23 dye. Ceramics International, 2015, 41, 7773-7782.	2.3	150
16	Photocatalysis from UV/Vis to Nearâ€Infrared Light: Towards Full Solarâ€Light Spectrum Activity. ChemCatChem, 2015, 7, 559-573.	1.8	148
17	Novel Preparation of Anatase TiO <sub>2</sub> @Reduced Graphene Oxide Hybrids for High-Performance Dye-Sensitized Solar Cells. ACS Applied Materials & Interfaces, 2013, 5, 6635-6642.	4.0	147
18	CuO nanosheets as potential scaffolds for gas sensing applications. Sensors and Actuators B: Chemical, 2017, 250, 24-31.	4.0	137

#	Article	IF	CITATIONS
19	Controlled synthesis of various ZnO nanostructured materials by capping agents-assisted hydrothermal method for dye-sensitized solar cells. Electrochimica Acta, 2008, 53, 7869-7874.	2.6	132
20	Facile synthesis and optical properties of Co3O4 nanostructures by the microwave route. Superlattices and Microstructures, 2011, 49, 416-421.	1.4	131
21	Sulfamic Acid-Doped Polyaniline Nanofibers Thin Film-Based Counter Electrode: Application in Dye-Sensitized Solar Cells. Journal of Physical Chemistry C, 2010, 114, 4760-4764.	1.5	129
22	Ethanol chemi-sensor: Evaluation of structural, optical and sensing properties of CuO nanosheets. Materials Letters, 2011, 65, 1400-1403.	1.3	127
23	Rapid photocatalytic degradation of crystal violet dye over ZnO flower nanomaterials. Materials Letters, 2013, 96, 228-232.	1.3	124
24	Photocatalytic degradation of Eriochrome Black T dye using well-crystalline anatase TiO2 nanoparticles. Journal of Alloys and Compounds, 2013, 581, 392-397.	2.8	123
25	Ultra-sensitive hydrazine chemical sensor based on high-aspect-ratio ZnO nanowires. Talanta, 2009, 77, 1376-1380.	2.9	121
26	An effective nanocomposite of polyaniline and ZnO: preparation, characterizations, and its photocatalytic activity. Colloid and Polymer Science, 2011, 289, 415-421.	1.0	118
27	Hydrazine chemical sensing by modified electrode based on in situ electrochemically synthesized polyaniline/graphene composite thin film. Sensors and Actuators B: Chemical, 2012, 173, 177-183.	4.0	108
28	Synthesis, Characterization and Effect of pH Variation on Zinc Oxide Nanostructures. Materials Transactions, 2009, 50, 2092-2097.	0.4	107
29	The visible light-driven photocatalytic degradation of Alizarin red S using Bi-doped TiO <sub>2</sub> nanoparticles. New Journal of Chemistry, 2014, 38, 3127-3136.	1.4	107
30	Large-scale synthesis of ZnO balls made of fluffy thin nanosheets by simple solution process: Structural, optical and photocatalytic properties. Journal of Colloid and Interface Science, 2011, 363, 521-528.	5.0	103
31	Advances in Responsively Conductive Polymer Composites and Sensing Applications. Polymer Reviews, 2021, 61, 157-193.	5.3	103
32	Recent Advances and Perspectives of Carbon-Based Nanostructures as Anode Materials for Li-ion Batteries. Materials, 2019, 12, 1229.	1.3	102
33	Well-crystalline porous ZnO–SnO2 nanosheets: An effective visible-light driven photocatalyst and highly sensitive smart sensor material. Talanta, 2015, 131, 490-498.	2.9	100
34	Growth and properties of Ag-doped ZnO nanoflowers for highly sensitive phenyl hydrazine chemical sensor application. Talanta, 2012, 93, 257-263.	2.9	99
35	Sonophotocatalytic degradation of methyl orange using ZnO nano-aggregates. Journal of Alloys and Compounds, 2015, 629, 167-172.	2.8	98
36	Solvent-free graphene liquids: Promising candidates for lubricants without the base oil. Journal of Colloid and Interface Science, 2019, 542, 159-167.	5.0	98

#	Article	IF	CITATIONS
37	Ce-doped ZnO nanorods for the detection of hazardous chemical. Sensors and Actuators B: Chemical, 2012, 173, 72-78.	4.0	97
38	Synthesis, characterization and acetone gas sensing applications of Ag-doped ZnO nanoneedles. Ceramics International, 2017, 43, 6765-6770.	2.3	97
39	Growth and properties of well-crystalline cerium oxide (CeO2) nanoflakes for environmental and sensor applications. Journal of Colloid and Interface Science, 2015, 454, 61-68.	5.0	94
40	Photocatalytic degradation of Alizarin Red S using simply synthesized ZnO nanoparticles. Materials Letters, 2013, 106, 385-389.	1.3	93
41	Photocatalytic degradation of the antibiotic levofloxacin using highly crystalline TiO <sub>2</sub> nanoparticles. New Journal of Chemistry, 2014, 38, 3220-3226.	1.4	93
42	Cross-linking of dialdehyde carboxymethyl cellulose with silk sericin to reinforce sericin film for potential biomedical application. Carbohydrate Polymers, 2019, 212, 403-411.	5.1	93
43	Water splitting on Rhodamine-B dye sensitized Co-doped TiO2 catalyst under visible light. Applied Catalysis B: Environmental, 2012, 111-112, 397-401.	10.8	92
44	Tungsten oxide (WO3) nanoparticles as scaffold for the fabrication of hydrazine chemical sensor. Sensors and Actuators B: Chemical, 2014, 196, 231-237.	4.0	92
45	Synthesis of CeO2–ZnO nanoellipsoids as potential scaffold for the efficient detection of 4-nitrophenol. Sensors and Actuators B: Chemical, 2014, 202, 1044-1050.	4.0	92
46	Effect of annealing temperature on the properties and photocatalytic efficiencies of ZnO nanoparticles. Journal of Alloys and Compounds, 2015, 648, 46-52.	2.8	92
47	Enhanced photoresponse under visible light in Pt ionized TiO2 nanotube for the photocatalytic splitting of water. Catalysis Communications, 2008, 10, 1-5.	1.6	90
48	Ultra-high sensitive ammonia chemical sensor based on ZnO nanopencils. Talanta, 2012, 89, 155-161.	2.9	89
49	ZnO doped SnO2 nanoparticles heterojunction photo-catalyst for environmental remediation. Journal of Alloys and Compounds, 2015, 653, 327-333.	2.8	89
50	Advanced ZnO–graphene oxide nanohybrid and its photocatalytic Applications. Materials Letters, 2013, 100, 261-265.	1.3	88
51	Green synthesis of Co3O4 nanoparticles and their applications in thermal decomposition of ammonium perchlorate and dye-sensitized solar cells. Materials Science and Engineering B: Solid-State Materials for Advanced Technology, 2015, 193, 181-188.	1.7	88
52	Three-Dimensional Crumpled Graphene-Based Nanosheets with Ultrahigh NO <sub>2</sub> Gas Sensibility. ACS Applied Materials & Interfaces, 2017, 9, 11819-11827.	4.0	88
53	Solar light driven photocatalytic degradation of levofloxacin using TiO <sub>2</sub> /carbon-dot nanocomposites. New Journal of Chemistry, 2018, 42, 7445-7456.	1.4	87
54	Vertically Aligned ZnO Nanorods on Hot Filament Chemical Vapor Deposition Grown Graphene Oxide Thin Film Substrate: Solar Energy Conversion. ACS Applied Materials & Interfaces, 2012, 4, 4405-4412.	4.0	85

#	Article	IF	CITATIONS
55	Fabrication and characterization of highly sensitive and selective sensors based on porous NiO nanodisks. Sensors and Actuators B: Chemical, 2018, 259, 604-615.	4.0	85
56	Growth of Comb-like ZnO Nanostructures for Dye-sensitized Solar Cells Applications. Nanoscale Research Letters, 2009, 4, 1004-1008.	3.1	84
57	CeO2ZnO hexagonal nanodisks: Efficient material for the degradation of direct blue 15 dye and its simulated dye bath effluent under solar light. Journal of Alloys and Compounds, 2015, 620, 67-73.	2.8	84
58	TiO2 quantum dots for the photocatalytic degradation of indigo carmine dye. Journal of Alloys and Compounds, 2015, 650, 193-198.	2.8	83
59	NiCo <sub>2</sub> O <sub>4</sub> nanowire based flexible electrode materials for asymmetric supercapacitors. New Journal of Chemistry, 2018, 42, 7399-7406.	1.4	83
60	Cobalt oxide nanocubes as electrode material for the performance evaluation of electrochemical supercapacitor. Ceramics International, 2018, 44, 588-595.	2.3	83
61	A Review on Synthesis Processing, Chemical and Conduction Properties of Polyaniline and Its Nanocomposites. Science of Advanced Materials, 2010, 2, 441-462.	0.1	83
62	Growth, properties and dye-sensitized solar cells–applications of ZnO nanorods grown by low-temperature solution process. Superlattices and Microstructures, 2009, 45, 529-534.	1.4	82
63	2D Sn-doped ZnO ultrathin nanosheet networks for enhanced acetone gas sensing application. Ceramics International, 2017, 43, 2418-2423.	2.3	81
64	An Insight into Atmospheric Plasma Jet Modified ZnO Quantum Dots Thin Film for Flexible Perovskite Solar Cell: Optoelectronic Transient and Charge Trapping Studies. Journal of Physical Chemistry C, 2015, 119, 10379-10390.	1.5	80
65	Zinc oxide nanostructure-based dye-sensitized solar cells. Journal of Materials Science, 2017, 52, 4743-4795.	1.7	79
66	Mimicking a Dog's Nose: Scrolling Graphene Nanosheets. ACS Nano, 2018, 12, 2521-2530.	7.3	78
67	MgO polyhedral nanocages and nanocrystals based glucose biosensor. Electrochemistry Communications, 2009, 11, 1353-1357.	2.3	77
68	Nanocomposites of poly(1-naphthylamine)/SiO2 and poly(1-naphthylamine)/TiO2: Comparative photocatalytic activity evaluation towards methylene blue dye. Applied Catalysis B: Environmental, 2011, 103, 136-142.	10.8	77
69	Enhanced photocatalytic degradation of harmful dye and phenyl hydrazine chemical sensing using ZnO nanourchins. Chemical Engineering Journal, 2015, 262, 588-596.	6.6	76
70	A highly sensitive ammonia chemical sensor based on α-Fe <sub>2</sub> O <sub>3</sub> nanoellipsoids. Journal Physics D: Applied Physics, 2011, 44, 425401.	1.3	75
71	Highly sensitive hydrazine chemical sensor fabricated by modified electrode of vertically aligned zinc oxide nanorods. Talanta, 2012, 100, 377-383.	2.9	75
72	Architecture-controlled synthesis of M <sub>x</sub> O <sub>y</sub> (M = Ni, Fe, Cu) microfibres from seaweed biomass for high-performance lithium ion battery anodes. Journal of Materials Chemistry A, 2015, 3, 22708-22715.	5.2	75

#	Article	IF	CITATIONS
73	Layered double hydroxide/graphene oxide hybrid incorporated polysulfone substrate for thin-film nanocomposite forward osmosis membranes. RSC Advances, 2016, 6, 56599-56609.	1.7	75
74	Bi2WO6/C-Dots/TiO2: A Novel Z-Scheme Photocatalyst for the Degradation of Fluoroquinolone Levofloxacin from Aqueous Medium. Nanomaterials, 2020, 10, 910.	1.9	75
75	Sno2 quantum dots as novel platform for electrochemical sensing of cadmium. Electrochimica Acta, 2015, 169, 97-102.	2.6	74
76	Rapid Solar-Light Driven Superior Photocatalytic Degradation of Methylene Blue Using MoS2-ZnO Heterostructure Nanorods Photocatalyst. Materials, 2018, 11, 2254.	1.3	74
77	Reduced graphene/nanostructured cobalt oxide nanocomposite for enhanced electrochemical performance of supercapacitor applications. Journal of Colloid and Interface Science, 2020, 558, 68-77.	5.0	74
78	2D Nanomaterial-Based Surface Plasmon Resonance Sensors for Biosensing Applications. Micromachines, 2020, 11, 779.	1.4	74
79	Hydrothermally grown ZnO nanoflowers for environmental remediation and clean energy applications. Materials Research Bulletin, 2012, 47, 2407-2414.	2.7	73
80	Ag-doped ZnO nanoellipsoids: Potential scaffold for photocatalytic and sensing applications. Talanta, 2015, 137, 204-213.	2.9	73
81	Synthesis, characterization and application of sol–gel derived mesoporous TiO2 nanoparticles for dye-sensitized solar cells. Solar Energy, 2010, 84, 2195-2201.	2.9	72
82	Enhanced electrochemical activity of low temperature solution process synthesized Co3O4 nanoparticles for pseudo-supercapacitors applications. Ceramics International, 2016, 42, 1879-1885.	2.3	72
83	Phytoconstituents assisted green synthesis of cerium oxide nanoparticles for thermal decomposition and dye remediation. Materials Research Bulletin, 2017, 91, 98-107.	2.7	72
84	Enhanced visible light driven photocatalytic application of Ag 2 O decorated ZnO nanorods heterostructures. Separation and Purification Technology, 2017, 183, 341-349.	3.9	72
85	Visible-light-driven photocatalytic and chemical sensing properties of SnS2 nanoflakes. Talanta, 2013, 114, 183-190.	2.9	71
86	Carbon nanotubes–polyethylene oxide composite electrolyte for solid-state dye-sensitized solar cells. Electrochimica Acta, 2010, 55, 2418-2423.	2.6	70
87	Highly sensitive p-nitrophenol chemical sensor based on crystalline α-MnO <sub>2</sub> nanotubes. New Journal of Chemistry, 2014, 38, 4420-4426.	1.4	70
88	Fabrication and characterization of highly sensitive and selective arsenic sensor based on ultra-thin graphene oxide nanosheets. Sensors and Actuators B: Chemical, 2016, 227, 29-34.	4.0	70
89	Catalytic thermal decomposition of ammonium perchlorate and combustion of composite solid propellants over green synthesized CuO nanoparticles. Thermochimica Acta, 2015, 614, 110-115.	1.2	66
90	Sunlight-driven photocatalytic degradation of non-steroidal anti-inflammatory drug based on TiO2 quantum dots. Journal of Colloid and Interface Science, 2015, 459, 257-263.	5.0	66

#	Article	IF	CITATIONS
91	Effective NiCu NPs-doped carbon nanofibers as counter electrodes for dye-sensitized solar cells. Electrochimica Acta, 2013, 102, 142-148.	2.6	65
92	Statistical analysis of gold nanoparticle-induced oxidative stress and apoptosis in myoblast (C2C12) cells. Colloids and Surfaces B: Biointerfaces, 2014, 123, 664-672.	2.5	65
93	High performance of NiCo nanoparticles-doped carbon nanofibers as counter electrode for dye-sensitized solar cells. Electrochimica Acta, 2015, 160, 1-6.	2.6	64
94	Graphitic carbon nitride (g-C <sub>3</sub> N <sub>4</sub> ) coated titanium oxide nanotube arrays with enhanced photo-electrochemical performance. Dalton Transactions, 2016, 45, 12702-12709.	1.6	64
95	Structural and optical properties of CuO layered hexagonal discs synthesized by a low-temperature hydrothermal process. Journal Physics D: Applied Physics, 2011, 44, 155405.	1.3	63
96	Enhanced Photocatalytic Activity of B, N-Codoped TiO <sub>2</sub> by a New Molten Nitrate Process. Journal of Nanoscience and Nanotechnology, 2019, 19, 839-849.	0.9	63
97	Communication—Ultra-Small NiO Nanoparticles Grown by Low-Temperature Process for Electrochemical Application. Journal of the Electrochemical Society, 2020, 167, 167517.	1.3	63
98	NiO nanodisks: Highly efficient visible-light driven photocatalyst, potential scaffold for seed germination of Vigna Radiata and antibacterial properties. Journal of Cleaner Production, 2018, 190, 563-576.	4.6	62
99	Synthesis of polypropylene/Mg3Al–X (X = CO32â~', NO3â^', Clâ^', SO42â~') LDH nanocomposites using a solvent mixing method: thermal and melt rheological properties. Journal of Materials Chemistry A, 2013, 1, 9928.	5.2	61
100	Zinc Oxide Nanomaterials for Photocatalytic Degradation of Methyl Orange: A Review. Nanoscience and Nanotechnology Letters, 2014, 6, 631-650.	0.4	60
101	Azadirachta indica plant-assisted green synthesis of Mn3O4 nanoparticles: Excellent thermal catalytic performance and chemical sensing behavior. Journal of Colloid and Interface Science, 2016, 472, 220-228.	5.0	60
102	Visible light driven photocatalytic degradation of fluoroquinolone levofloxacin drug using Ag <sub>2</sub> O/TiO <sub>2</sub> quantum dots: a mechanistic study and degradation pathway. New Journal of Chemistry, 2017, 41, 12079-12090.	1.4	60
103	Two-dimensional ytterbium oxide nanodisks based biosensor for selective detection of urea. Biosensors and Bioelectronics, 2017, 98, 254-260.	5.3	59
104	Low-temperature synthesis of α-Fe2O3 hexagonal nanoparticles for environmental remediation and smart sensor applications. Talanta, 2013, 116, 1060-1066.	2.9	58
105	Silica-Based Bioactive Glasses and Their Applications in Hard Tissue Regeneration: A Review. Pharmaceuticals, 2021, 14, 75.	1.7	58
106	Fabrication and growth mechanism of hexagonal zinc oxide nanorods via solution process. Journal of Materials Science, 2010, 45, 2967-2973.	1.7	57
107	Microwave assisted rapid growth of Mg(OH)2 nanosheet networks for ethanol chemical sensor application. Journal of Alloys and Compounds, 2012, 519, 4-8.	2.8	57
108	Growth and characterization of nanospikes decorated ZnO sheets and their solar cell application. Chemical Engineering Journal, 2012, 195-196, 307-313.	6.6	56

#	Article	IF	CITATIONS
109	Fabrication and characterization of CuO nanoplates based sensor device for ethanol gas sensing application. Chemical Physics Letters, 2021, 763, 138204.	1.2	56
110	Formation of SiC nanowhiskers by carbothermic reduction of silica with activated carbon. Materials Letters, 2009, 63, 174-176.	1.3	55
111	Pd–Co-doped carbon nanofibers with photoactivity as effective counter electrodes for DSSCs. Chemical Engineering Journal, 2012, 211-212, 9-15.	6.6	55
112	Demonstrated photons to electron activity of S-doped TiO 2 nanofibers as photoanode in the DSSC. Materials Letters, 2018, 225, 77-81.	1.3	55
113	Urea sensor based on tin oxide thin films prepared by modified plasma enhanced CVD. Sensors and Actuators B: Chemical, 2008, 132, 265-271.	4.0	54
114	Ultra-sensitive ethanol sensor based on rapidly synthesized Mg(OH)2 hexagonal nanodisks. Sensors and Actuators B: Chemical, 2012, 166-167, 97-102.	4.0	54
115	High efficiency solid state dye sensitized solar cells with graphene–polyethylene oxide composite electrolytes. Nanoscale, 2013, 5, 5403.	2.8	54
116	Supramolecularly Modified Graphene for Ultrafast Responsive and Highly Stable Humidity Sensor. Journal of Physical Chemistry C, 2015, 119, 28640-28647.	1.5	54
117	Evaluation of novel indigenous fungal consortium for enhanced bioremediation of heavy metals from contaminated sites. Environmental Technology and Innovation, 2020, 20, 101050.	3.0	54
118	Hierarchical Fe <sub>3</sub> O <sub>4</sub> Core–Shell Layered Double Hydroxide Composites as Magnetic Adsorbents for Anionic Dye Removal from Wastewater. European Journal of Inorganic Chemistry, 2015, 2015, 4182-4191.	1.0	53
119	Supercapacitors with ultrahigh energy density based on mesoporous carbon nanofibers: Enhanced double-layer electrochemical properties. Journal of Alloys and Compounds, 2015, 653, 212-218.	2.8	53
120	Sm2O3-doped ZnO beech fern hierarchical structures for nitroaniline chemical sensor. Ceramics International, 2016, 42, 16505-16511.	2.3	53
121	ZnO Nanorods Based Hydrazine Sensors. Journal of Nanoscience and Nanotechnology, 2009, 9, 4686-4691.	0.9	52
122	Fabrication of Highly Sensitive Non-Enzymatic Glucose Biosensor Based on ZnO Nanorods. Science of Advanced Materials, 2011, 3, 901-906.	0.1	52
123	Toward a high performance asymmetric hybrid capacitor by electrode optimization. Inorganic Chemistry Frontiers, 2019, 6, 2824-2831.	3.0	52
124	Synthesis and characterization of novel poly(1-naphthylamine)/zinc oxide nanocomposites: Application in catalytic degradation of methylene blue dye. Colloid and Polymer Science, 2010, 288, 1633-1638.	1.0	51
125	High-Efficiency Electrode Based on Nitrogen-Doped TiO2 Nanofibers for Dye-Sensitized Solar Cells. Electrochimica Acta, 2014, 115, 493-498.	2.6	51
126	Chemical and Pathogenic Cleanup of Wastewater Using Surface-Functionalized CeO <sub>2</sub> Nanoparticles. ACS Sustainable Chemistry and Engineering, 2017, 5, 6803-6816.	3.2	51

#	Article	IF	CITATIONS
127	Transformation of solid plastic waste to activated carbon fibres for wastewater treatment. Chemosphere, 2022, 294, 133692.	4.2	51
128	Predominance of two dimensional (2D) Mn2O3 nanowalls thin film for high performance electrochemical supercapacitors. Chemical Engineering Journal, 2017, 330, 1240-1247.	6.6	50
129	Synthesis and electrochemical impedance properties of CdS nanoparticles decorated polyaniline nanorods. Chemical Engineering Journal, 2012, 181-182, 806-812.	6.6	49
130	Biosynthesized NiO nanoparticles: Potential catalyst for ammonium perchlorate and composite solid propellants. Ceramics International, 2015, 41, 1573-1578.	2.3	49
131	Composite electrolyte of heteropolyacid (HPA) and polyethylene oxide (PEO) for solid-state dye-sensitized solar cell. Electrochimica Acta, 2008, 53, 6623-6628.	2.6	48
132	Zinc oxide nanocones as potential scaffold for the fabrication of ultra-high sensitive hydrazine chemical sensor. Ceramics International, 2015, 41, 3101-3108.	2.3	47
133	Engineering of magnetically separable ZnFe2O4@ TiO2 nanofibers for dye-sensitized solar cells and removal of pollutant from water. Journal of Alloys and Compounds, 2017, 723, 477-483.	2.8	47
134	CuO Nanocubes Based Highly-Sensitive 4-Nitrophenol Chemical Sensor. Science of Advanced Materials, 2012, 4, 893-900.	0.1	47
135	Graphene application as a counter electrode material for dye-sensitized solar cell. Materials Letters, 2012, 86, 96-99.	1.3	46
136	Effect of graphene oxide ratio on the cell adhesion and growth behavior on a graphene oxide-coated silicon substrate. Scientific Reports, 2016, 6, 33835.	1.6	46
137	Microwave-assisted synthesis of ZnO doped CeO2 nanoparticles as potential scaffold for highly sensitive nitroaniline chemical sensor. Ceramics International, 2016, 42, 11562-11567.	2.3	46
138	Synthesis and Characterizations of Cd-Doped ZnO Multipods for Environmental Remediation Application. Journal of Nanoscience and Nanotechnology, 2012, 12, 8453-8458.	0.9	45
139	Ag/CeO2 nanostructured materials for enhanced photocatalytic and antibacterial applications. Ceramics International, 2019, 45, 20509-20517.	2.3	45
140	Development of Highly Sensitive and Selective Cholesterol Biosensor Based on Cholesterol Oxidase Co-Immobilized with α-Fe2O3 Micro-Pine Shaped Hierarchical Structures. Electrochimica Acta, 2014, 135, 396-403.	2.6	44
141	Solar light driven enhanced photocatalytic degradation of brilliant green dye based on ZnS quantum dots. Superlattices and Microstructures, 2017, 103, 365-375.	1.4	44
142	Low temperature solution processed Mn3O4 nanoparticles: Enhanced performance of electrochemical supercapacitors. Journal of Alloys and Compounds, 2017, 694, 560-567.	2.8	44
143	Ag-Doped ZnO Nanoparticles for Enhanced Ethanol Gas Sensing Application. Journal of Nanoscience and Nanotechnology, 2018, 18, 3557-3562.	0.9	44
144	Morphological and Electrochemical Properties of Crystalline Praseodymium Oxide Nanorods. Nanoscale Research Letters, 2010, 5, 735-740.	3.1	43

#	Article	IF	CITATIONS
145	Bismuth sulfide (Bi2S3) nanotubes decorated TiO2 nanoparticles heterojunction assembly for enhanced solar light driven photocatalytic activity. Ceramics International, 2016, 42, 17551-17557.	2.3	43
146	Zinc oxide quantum dots: multifunctional candidates for arresting C2C12 cancer cells and their role towards caspase 3 and 7 genes. RSC Advances, 2016, 6, 26111-26120.	1.7	43
147	High-efficiency dye-sensitized solar cells based on nitrogen and graphene oxide co-incorporated TiO2 nanofibers photoelectrode. Chemical Engineering Journal, 2015, 268, 153-161.	6.6	42
148	A Rapid Synthesis of Mesoporous Mn2O3 Nanoparticles for Supercapacitor Applications. Coatings, 2019, 9, 631.	1.2	42
149	Adsorptive removal of antibiotic ofloxacin in aqueous phase using rGO-MoS2 heterostructure. Journal of Hazardous Materials, 2021, 417, 125982.	6.5	42
150	CdO–ZnO nanorices for enhanced and selective formaldehyde gas sensing applications. Environmental Research, 2021, 200, 111377.	3.7	42
151	Plasma-enhanced polymerized aniline/TiO2 dye-sensitized solar cells. Journal of Alloys and Compounds, 2009, 487, 382-386.	2.8	41
152	ZnO nanocapsules for photocatalytic degradation of thionine. Materials Letters, 2012, 81, 239-241.	1.3	41
153	Electrochemical enzyme-less urea sensor based on nano-tin oxide synthesized by hydrothermal technique. Chemico-Biological Interactions, 2015, 242, 45-49.	1.7	41
154	An effective and low cost Pd Ce bimetallic decorated carbon nanofibers as electro-catalyst for direct methanol fuel cells applications. Journal of Alloys and Compounds, 2016, 684, 524-529.	2.8	41
155	Improvement in the surface properties of activated carbon via steam pretreatment for high performance supercapacitors. Applied Surface Science, 2017, 404, 88-93.	3.1	41
156	Electrochemical Investigations of Hydrothermally Synthesized Porous Cobalt Oxide (Co <sub>3</sub> ) Tj ETQq0	000.rgBT	/Overlock 10
157	Growth Mechanism and Optical Properties of Aligned Hexagonal ZnO Nanoprisms Synthesized by Noncatalytic Thermal Evaporation. Inorganic Chemistry, 2008, 47, 4088-4094.	1.9	40
158	Influence of seed layer treatment on low temperature grown ZnO nanotubes: Performances in dye sensitized solar cells. Electrochimica Acta, 2011, 56, 1111-1116.	2.6	40
159	Study on photocatalytic activity of ZnO nanodisks for the degradation of Rhodamine B dye. Materials Letters, 2015, 159, 265-268.	1.3	40
160	High-Yield Synthesis of Well-Crystalline <i>α</i> -Fe <sub>2</sub> O <sub>3</sub> Nanoparticles: Structural, Optical and Photocatalytic Properties. Journal of Nanoscience and Nanotechnology, 2011, 11, 3474-3480.	0.9	39
161	Polypropylene/Mg3Al–tartrazine LDH nanocomposites with enhanced thermal stability, UV absorption, and rheological properties. RSC Advances, 2013, 3, 26017.	1.7	39
162	Low temperature HFCVD synthesis of tungsten oxide thin film for high response hydrogen gas sensor application. Materials Letters, 2019, 254, 398-401.	1.3	39

#	Article	IF	CITATIONS
163	ZnO–SnO2 nanocubes for fluorescence sensing and dye degradation applications. Ceramics International, 2021, 47, 6201-6210.	2.3	39
164	Recycling of Waste Poly(ethylene terephthalate) Bottles by Alkaline Hydrolysis and Recovery of Pure Nanospindle-Shaped Terephthalic Acid. Journal of Nanoscience and Nanotechnology, 2018, 18, 5804-5809.	0.9	38
165	A simulation approach for investigating the performances of cadmium telluride solar cells using doping concentrations, carrier lifetimes, thickness of layers, and band gaps. Solar Energy, 2021, 216, 259-265.	2.9	38
166	Application of single walled carbon nanotubes as counter electrode for dye sensitized solar cells. Electrochimica Acta, 2012, 85, 600-604.	2.6	37
167	α-Fe <sub>2</sub> O <sub>3</sub> hexagonal cones synthesized from the leaf extract of Azadirachta indica and its thermal catalytic activity. New Journal of Chemistry, 2015, 39, 7105-7111.	1.4	37
168	Influence of GO incorporation in TiO2 nanofibers on the electrode efficiency in dye-sensitized solar cells. Ceramics International, 2015, 41, 1205-1212.	2.3	37
169	Ni Foam Substrates Modified with a ZnCo <sub>2</sub> O <sub>4</sub> Nanowire-Coated Ni(OH) <sub>2</sub> Nanosheet Electrode for Hybrid Capacitors and Electrocatalysts. ACS Applied Nano Materials, 2021, 4, 5461-5468.	2.4	37
170	New counter electrode of hot filament chemical vapor deposited graphene thin film for dye sensitized solar cell. Chemical Engineering Journal, 2013, 222, 464-471.	6.6	36
171	Structure modification of anatase TiO2 nanomaterials-based photoanodes for efficient dye-sensitized solar cells. Electrochimica Acta, 2013, 113, 527-535.	2.6	36
172	Cauliflower-shaped ZnO nanomaterials for electrochemical sensing and photocatalytic applications. Electrochimica Acta, 2016, 222, 463-472.	2.6	36
173	Fabrication and in-vitro biocompatibility of freeze-dried CTS-nHA and CTS-nBG scaffolds for bone regeneration applications. International Journal of Biological Macromolecules, 2020, 149, 1-10.	3.6	36
174	Photocurrent Induced by Conducting Channels of Hole Transporting Layer to Adjacent Photoactive Perovskite Sensitized TiO <sub>2</sub> Thin Film: Solar Cell Paradigm. Langmuir, 2014, 30, 12786-12794.	1.6	35
175	Fabrication and characterization of a highly sensitive hydroquinone chemical sensor based on iron-doped ZnO nanorods. Dalton Transactions, 2015, 44, 21081-21087.	1.6	35
176	Direct in situ synthesis of Fe2O3-codoped N-doped TiO2 nanoparticles with enhanced photocatalytic and photo-electrochemical properties. Journal of Alloys and Compounds, 2017, 705, 89-97.	2.8	35
177	Stable perovskite solar cells using thiazolo [5,4-d]thiazole-core containing hole transporting material. Nano Energy, 2018, 49, 372-379.	8.2	35
178	Highly sensitive and selective 2-nitroaniline chemical sensor based on Ce-doped SnO2 nanosheets/Nafion-modified glassy carbon electrode. Advanced Composites and Hybrid Materials, 2021, 4, 1015-1026.	9.9	35
179	Synthesis, characterization and performance as a Counter Electrode for dye-sensitized solar cells of CoCr-decorated carbon nanofibers. Ceramics International, 2016, 42, 146-153.	2.3	34
180	Nanocuboidal-shaped zirconium based metal organic framework for the enhanced adsorptive removal of nonsteroidal anti-inflammatory drug, ketorolac tromethamine, from aqueous phase. New Journal of Chemistry, 2018, 42, 1921-1930.	1.4	34

#	Article	IF	CITATIONS
181	All-Dry Transferred ReS <sub>2</sub> Nanosheets for Ultrasensitive Room-Temperature NO <sub>2</sub> Sensing under Visible Light Illumination. ACS Sensors, 2020, 5, 3172-3181.	4.0	34
182	An efficient chemical sensor based on CeO2 nanoparticles for the detection of acetylacetone chemical. Journal of Electroanalytical Chemistry, 2020, 864, 114089.	1.9	34
183	Effect of annealing on the conversion of ZnS to ZnO nanoparticles synthesized by the sol-gel method using zinc acetate and thiourea. Metals and Materials International, 2009, 15, 453-458.	1.8	33
184	Polyaniline/gallium doped ZnO heterostructure device via plasma enhanced polymerization technique: Preparation, characterization and electrical properties. Mikrochimica Acta, 2011, 172, 471-478.	2.5	33
185	Low cost sol–gel derived SiC–SiO2 nanocomposite as anti reflection layer for enhanced performance of crystalline silicon solar cells. Applied Surface Science, 2016, 369, 545-551.	3.1	33
186	A Highly-Sensitive Picric Acid Chemical Sensor Based on ZnO Nanopeanuts. Materials, 2017, 10, 795.	1.3	33
187	Composite CdO-ZnO hexagonal nanocones: Efficient materials for photovoltaic and sensing applications. Ceramics International, 2018, 44, 5017-5024.	2.3	33
188	Fabrication of Sericin/Agrose Gel Loaded Lysozyme and Its Potential in Wound Dressing Application. Nanomaterials, 2018, 8, 235.	1.9	33
189	Iron-nickel co-doped ZnO nanoparticles as scaffold for field effect transistor sensor: Application in electrochemical detection of hexahydropyridine chemical. Sensors and Actuators B: Chemical, 2018, 275, 422-431.	4.0	33
190	Effect of cerium ions in Ce-Doped ZnO nanostructures on their photocatalytic and picric acid chemical sensing. Ceramics International, 2021, 47, 3089-3098.	2.3	33
191	A new carbon nanotubes (CNTs)–poly acrylonitrile (PAN) composite electrolyte for solid state dye sensitized solar cells. Electrochimica Acta, 2011, 56, 9973-9979.	2.6	32
192	Structural, morphological and sensing properties of layered polyaniline nanosheets towards hazardous phenol chemical. Talanta, 2013, 104, 219-227.	2.9	32
193	Template-free growth of well-crystalline α-Fe2O3 nanopeanuts with enhanced visible-light driven photocatalytic properties. Journal of Colloid and Interface Science, 2015, 457, 345-352.	5.0	32
194	Nanocages-augmented aligned polyaniline nanowires as unique platform for electrochemical non-enzymatic glucose biosensor. Applied Catalysis A: General, 2016, 517, 21-29.	2.2	32
195	A Novel AgNPs/Sericin/Agar Film with Enhanced Mechanical Property and Antibacterial Capability. Molecules, 2018, 23, 1821.	1.7	32
196	Bioremediation potential of novel fungal species isolated from wastewater for the removal of lead from liquid medium. Environmental Technology and Innovation, 2020, 18, 100757.	3.0	32
197	NiCu bimetallic nanoparticle-decorated graphene as novel and cost-effective counter electrode for dye-sensitized solar cells and electrocatalyst for methanol oxidation. Applied Catalysis A: General, 2015, 501, 41-47.	2.2	31
198	A symmetric benzoselenadiazole based D–A–D small molecule for solution processed bulk-heterojunction organic solar cells. Journal of Industrial and Engineering Chemistry, 2020, 81, 309-316.	2.9	31

#	Article	IF	CITATIONS
199	Enhanced NO2 gas sensor device based on supramolecularly assembled polyaniline/silver oxide/graphene oxide composites. Ceramics International, 2021, 47, 25696-25707.	2.3	31
200	Exclusion of metal oxide by an RF sputtered Ti layer in flexible perovskite solar cells: energetic interface between a Ti layer and an organic charge transporting layer. Dalton Transactions, 2015, 44, 6439-6448.	1.6	30
201	Visible-light-driven photocatalytic properties of simply synthesized α-Iron(III)oxide nanourchins. Journal of Colloid and Interface Science, 2015, 451, 93-100.	5.0	30
202	Highly dense ZnO nanowhiskers for the low level detection of p-hydroquinone. Materials Letters, 2015, 155, 82-86.	1.3	30
203	Significantly enhanced mechanical and electrical properties of epoxy nanocomposites reinforced with low loading of polyaniline nanoparticles. RSC Advances, 2016, 6, 21187-21192.	1.7	30
204	Vertically Arranged Zinc Oxide Nanorods as Antireflection Layer for Crystalline Silicon Solar Cell: A Simulation Study of Photovoltaic Properties. Applied Sciences (Switzerland), 2020, 10, 6062.	1.3	30
205	D-ï€-A-ï€-D type thiazolo[5,4-d]thiazole-core organic chromophore and graphene modified PEDOT:PSS buffer layer for efficient bulk heterojunction organic solar cells. Solar Energy, 2018, 171, 366-373.	2.9	29
206	Manipulating the Electrocatalytic Performance of NiCoP Nanowires by V Doping Under Acidic and Basic Conditions for Hydrogen and Oxygen Evolution Reactions. ACS Applied Nano Materials, 2021, 4, 10791-10798.	2.4	29
207	lodine doped polyaniline thin film for heterostructure devices via PECVD technique: Morphological, structural, and electrical properties. Macromolecular Research, 2012, 20, 30-36.	1.0	28
208	An electrochemical sensing platform based on hollow mesoporous ZnO nanoglobules modified glassy carbon electrode: Selective detection of piperidine chemical. Chemical Engineering Journal, 2015, 270, 564-571.	6.6	28
209	Immobilization interaction between xenobiotic and Bjerkandera adusta for the biodegradation of atrazine. Chemosphere, 2020, 257, 127060.	4.2	28
210	Platinum nanoparticles decorated carbon nanotubes for highly sensitive 2-nitrophenol chemical sensor. Ceramics International, 2016, 42, 9257-9263.	2.3	27
211	Wastewater cleanup using Phlebia acerina fungi: An insight into mycoremediation. Journal of Environmental Management, 2018, 228, 130-139.	3.8	27
212	Urchin like CuO hollow microspheres for selective high response ethanol sensor application: Experimental and theoretical studies. Ceramics International, 2021, 47, 12084-12095.	2.3	27
213	Utilization of ZnO Nanocones for the Photocatalytic Degradation of Acridine Orange. Journal of Nanoscience and Nanotechnology, 2011, 11, 4061-4066.	0.9	26
214	Lotus-leaf like ZnO nanostructures based electrode for the fabrication of ethyl acetate chemical sensor. Materials Letters, 2016, 164, 562-566.	1.3	26
215	Highly sensitive and selective non-enzymatic monosaccharide and disaccharide sugar sensing based on carbon paste electrodes modified with perforated NiO nanosheets. New Journal of Chemistry, 2018, 42, 964-973.	1.4	26
216	ZnO nanoflakes nanomaterials via hydrothermal process for dye sensitized solar cells. Materials Letters, 2018, 230, 92-95.	1.3	26

#	Article	IF	CITATIONS
217	Identification and characterization of cadmium resistant fungus isolated from contaminated site and its potential for bioremediation. Environmental Technology and Innovation, 2020, 17, 100604.	3.0	26
218	Synthesis and Characterization of ZnO Nanorods and Balls Nanomaterials for Dye Sensitized Solar Cells. Journal of Nanoengineering and Nanomanufacturing, 2011, 1, 71-76.	0.3	26
219	Low temperature grown ZnO nanotubes as smart sensing electrode for the effective detection of ethanolamine chemical. Materials Letters, 2013, 106, 254-258.	1.3	25
220	Electrochemical detection of resorcinol chemical using unique cabbage like ZnO nanostructures. Materials Letters, 2017, 209, 571-575.	1.3	25
221	In-Doped ZnO Hexagonal Stepped Nanorods and Nanodisks as Potential Scaffold for Highly-Sensitive Phenyl Hydrazine Chemical Sensors. Materials, 2017, 10, 1337.	1.3	25
222	Bare and nonionic surfactant-functionalized praseodymium oxide nanoparticles: Toxicological studies. Chemosphere, 2018, 209, 1007-1020.	4.2	25
223	Sol–Gel Deposited Double Layer TiO <sub>2</sub> and Al <sub>2</sub> O <sub>3</sub> Anti-Reflection Coating for Silicon Solar Cell. Journal of Nanoscience and Nanotechnology, 2018, 18, 1274-1278.	0.9	25
224	Polydopamine-Based Surface Modification of ZnO Nanoparticles on Sericin/Polyvinyl Alcohol Composite Film for Antibacterial Application. Molecules, 2019, 24, 503.	1.7	25
225	Fern shaped La2O3 nanostructures as potential scaffold for efficient hydroquinone chemical sensing application. Ceramics International, 2020, 46, 5141-5148.	2.3	25
226	Ultrasensitive and selective label-free aptasensor for the detection of penicillin based on nanoporous PtTi/graphene oxide-Fe3O4/ MWCNT-Fe3O4 nanocomposite. Microchemical Journal, 2020, 158, 105270.	2.3	25
227	Carbon Nanotube (CNT)–Polymethyl Methacrylate (PMMA) Composite Electrolyte for Solid-State Dye Sensitized Solar Cells. Journal of Nanoscience and Nanotechnology, 2010, 10, 3502-3507.	0.9	24
228	Effective modified electrode of poly (1-naphthylamine) nanoglobules for ultra-high sensitive ethanol chemical sensor. Chemical Engineering Journal, 2013, 229, 267-275.	6.6	24
229	Time dependent growth of ZnO nanoflowers with enhanced field emission properties. Ceramics International, 2016, 42, 13215-13222.	2.3	24
230	Speedy photocatalytic degradation of bromophenol dye over ZnO nanoflowers. Materials Letters, 2017, 209, 150-154.	1.3	24
231	Tuning electronic structures of thiazolo[5,4-d]thiazole-based hole-transporting materials for efficient perovskite solar cells. Solar Energy Materials and Solar Cells, 2018, 180, 334-342.	3.0	24
232	Nitroaniline chemi-sensor based on bitter gourd shaped ytterbium oxide (Yb2O3) doped zinc oxide (ZnO) nanostructures. Ceramics International, 2019, 45, 13825-13831.	2.3	24
233	Visible-Light Driven Photocatalytic Degradation of Eosin Yellow (EY) Dye Based on NiO-WO <sub>3</sub> Nanoparticles. Journal of Nanoscience and Nanotechnology, 2020, 20, 924-933.	0.9	24
234	A stable gel electrolyte based on poly butyl acrylate (PBA)-co-poly acrylonitrile (PAN) for solid-state dye-sensitized solar cells. Chemical Physics Letters, 2020, 754, 137756.	1.2	24

#	Article	IF	CITATIONS
235	Colloidal synthesis of NiMn2O4 nanodisks decorated reduced graphene oxide for electrochemical applications. Microchemical Journal, 2021, 160, 105630.	2.3	24
236	Photocatalytic and fluorescent chemical sensing applications of La-doped ZnO nanoparticles. Chemical Papers, 2021, 75, 1555-1566.	1.0	24
237	Synthesis of porous 2D layered nickel oxide-reduced graphene oxide (NiO-rGO) hybrid composite for the efficient electrochemical detection of epinephrine in biological fluid. Environmental Research, 2021, 200, 111366.	3.7	24
238	Photocatalytic Degradation of Direct Red-23 Dye with ZnO Nanoparticles. Journal of Nanoscience and Nanotechnology, 2014, 14, 7161-7166.	0.9	23
239	Biogenic Synthesis, Characterization and Evaluation of Silver Nanoparticles from Aspergillus niger JX556221 Against Human Colon Cancer Cell Line HT-29. Journal of Nanoscience and Nanotechnology, 2018, 18, 3673-3681.	0.9	23
240	Synergy of CO <sub>2</sub> Response and Aggregation-Induced Emission in a Block Copolymer: A Facile Way To "See―Cancer Cells. ACS Applied Materials & Interfaces, 2019, 11, 37077-37083.	4.0	23
241	Impact of porous Mn3O4 nanostructures on the performance of rechargeable lithium ion battery: Excellent capacity and cyclability. Solid State Ionics, 2019, 336, 31-38.	1.3	23
242	Multiple ions detection by field-effect transistor sensors based on ZnO@GO and ZnO@rGO nance and Compare and Compare and the sense of the compare and the comp	4.2	23
243	α-Bi2O3 nanosheets: An efficient material for sunlight-driven photocatalytic degradation of Rhodamine B. Ceramics International, 2022, 48, 29580-29588.	2.3	23
244	Morphology-dependent performance of Mg <sub>3</sub> Al–CO <sub>3</sub> layered double hydroxide as a nanofiller for polypropylene nanocomposites. RSC Advances, 2015, 5, 51900-51911.	1.7	22
245	Furan-bridged thiazolo [5,4-d]thiazole based D–ï€â€"A–ï€â€"D type linear chromophore for solution-processed bulk-heterojunction organic solar cells. RSC Advances, 2015, 5, 6286-6293.	1.7	22
246	Effect of Fluoride on the Morphology and Electrochemical Property of Co3O4 Nanostructures for Hydrazine Detection. Materials, 2018, 11, 207.	1.3	22
247	Rapid Growth of TiO2 Nanoflowers via Low-Temperature Solution Process: Photovoltaic and Sensing Applications. Materials, 2019, 12, 566.	1.3	22
248	Gas sensor device for high-performance ethanol sensing using α-MnO2 nanoparticles. Materials Letters, 2021, 286, 129232.	1.3	22
249	Sustainable removal of Ni(II) from waste water by freshly isolated fungal strains. Chemosphere, 2021, 282, 130871.	4.2	21
250	NO <i><sub>x</sub></i> Gas Sensing Properties of Fe-Doped ZnO Nanoparticles. Science of Advanced Materials, 2020, 12, 908-914.	0.1	21
251	Mineralization of rhodamine 6G dye over rose flower-like ZnO nanomaterials. Materials Letters, 2013, 113, 20-24.	1.3	20
252	Low Resistance Transparent Graphene-Like Carbon Thin Film Substrates for High Performance Dye Sensitized Solar Cells. Electrochimica Acta, 2014, 115, 559-565.	2.6	20

#	Article	IF	CITATIONS
253	ZnO quantum dots engrafted graphene oxide thin film electrode for low level detection of ethyl acetate. Materials Letters, 2014, 136, 379-383.	1.3	20
254	A comprehensive review on selective catalytic reduction catalysts for NO <sub>x</sub> emission abatement from municipal solid waste incinerators. Environmental Progress and Sustainable Energy, 2016, 35, 1061-1069.	1.3	20
255	Synthesis of Pt/K2CO3/MgAlOx–reduced graphene oxide hybrids as promising NOx storage–reduction catalytic performance. Scientific Reports, 2017, 7, 42862.	1.6	20
256	One-Step Fabrication of Pyranine Modified- Reduced Graphene Oxide with Ultrafast and Ultrahigh Humidity Response. Scientific Reports, 2017, 7, 2713.	1.6	20
257	Impact of Different Antireflection Layers on Cadmium Telluride (CdTe) Solar Cells: a PC1D Simulation Study. Journal of Electronic Materials, 2021, 50, 2199-2205.	1.0	20
258	Growth and formation mechanism of sea urchin-like ZnO nanostructures on Si. Korean Journal of Chemical Engineering, 2005, 22, 489-493.	1.2	19
259	Fabrication of polyaniline/ heterojunction structure using plasma enhanced polymerization technique. Superlattices and Microstructures, 2009, 46, 745-751.	1.4	19
260	Controlled synthesis and photoelectrochemical properties of highly ordered TiO2 nanorods. RSC Advances, 2012, 2, 4807.	1.7	19
261	Deployment of aligned ZnO nanorod with distinctive porous morphology: Potential scaffold for the detection of p-nitrophenylamine. Applied Catalysis A: General, 2014, 470, 271-277.	2.2	19
262	Supramolecular fabrication of polyelectrolyte-modified reduced graphene oxide for NO2 sensing applications. Ceramics International, 2015, 41, 12130-12136.	2.3	19
263	Preparation and Characterization of AgNPs In Situ Synthesis on Polyelectrolyte Membrane Coated Sericin/Agar Film for Antimicrobial Applications. Materials, 2018, 11, 1205.	1.3	19
264	Ethylene Glycol Functionalized Gadolinium Oxide Nanoparticles as a Potential Electrochemical Sensing Platform for Hydrazine and p-Nitrophenol. Coatings, 2019, 9, 633.	1.2	19
265	Label-Free Electrochemical Sensor Based on Manganese Doped Titanium Dioxide Nanoparticles for Myoglobin Detection: Biomarker for Acute Myocardial Infarction. Molecules, 2021, 26, 4252.	1.7	19
266	Effective removal of Pb(II) and Ni(II) ions by Bacillus cereus and Bacillus pumilus: An experimental and mechanistic approach. Environmental Research, 2022, 212, 113337.	3.7	19
267	TiO2 nanotube arrays <i>via</i> electrochemical anodic oxidation: Prospective electrode for sensing phenyl hydrazine. Applied Physics Letters, 2013, 103, .	1.5	18
268	Electrical properties of solution processed p-SnS nanosheets/n-TiO2 heterojunction assembly. Applied Physics Letters, 2013, 103, .	1.5	18
269	Hexagonal cadmium oxide nanodisks: Efficient scaffold for cyanide ion sensing and photo-catalytic applications. Talanta, 2016, 153, 57-65.	2.9	18
270	Iron-Doped Titanium Dioxide Nanoparticles As Potential Scaffold for Hydrazine Chemical Sensor Applications. Coatings, 2020, 10, 182.	1.2	18

#	Article	IF	CITATIONS
271	Numerical Investigation of Graphene as a Back Surface Field Layer on the Performance of Cadmium Telluride Solar Cell. Molecules, 2021, 26, 3275.	1.7	18
272	Direct sunlight-driven enhanced photocatalytic performance of V2O5 nanorods/ graphene oxide nanocomposites for the degradation of Victoria blue dye. Environmental Research, 2021, 199, 111369.	3.7	18
273	Highly porous ZnO nanosheets self-assembled in rosette-like morphologies for dye-sensitized solar cell application. New Journal of Chemistry, 2015, 39, 7961-7970.	1.4	17
274	Application of pristine and doped SnO2 nanoparticles as a matrix for agro-hazardous material (organophosphate) detection. Scientific Reports, 2017, 7, 42510.	1.6	17
275	Co <sub>3</sub> O <sub>4</sub> nanoparticles/MWCNTs composites: a potential scaffold for hydrazine and glucose electrochemical detection. RSC Advances, 2017, 7, 50087-50096.	1.7	17
276	The Influence of the Charge Compensating Anions of Layered Double Hydroxides (LDHs) in LDH-NS/Graphene Oxide Nanohybrid for CO <sub>2</sub> Capture. Journal of Nanoscience and Nanotechnology, 2018, 18, 2956-2964.	0.9	17
277	Enhanced solar light-mediated photocatalytic degradation of brilliant green dye in aqueous phase using BiPO4 nanospindles and MoS2/BiPO4 nanorods. Journal of Materials Science: Materials in Electronics, 2019, 30, 20741-20750.	1.1	17
278	Sunlight-Driven Photocatalytic Degradation of Methyl Orange Based on Bismuth Ferrite (BiFeO <sub>3</sub> ) Heterostructures Composed of Interconnected Nanosheets. Journal of Nanoscience and Nanotechnology, 2020, 20, 1851-1858.	0.9	17
279	Effect of Synthesis Temperature on the Morphologies, Optical and Electrical Properties of MgO Nanostructures. Journal of Nanoscience and Nanotechnology, 2020, 20, 2488-2494.	0.9	17
280	Delafossite CuCrO2 nanoparticles as possible electrode material for electrochemical supercapacitor. Ceramics International, 2022, 48, 16667-16676.	2.3	17
281	Effect of Deposition Temperature on the Growth of Yttriaâ€Stabilized Zirconia Thin Films on Si(111) by Chemical Vapor Deposition. Journal of the American Ceramic Society, 1999, 82, 2913-2915.	1.9	16
282	Hydrothermal synthesis of titanate nanotubes followed by electrodeposition process. Korean Journal of Chemical Engineering, 2006, 23, 1037-1045.	1.2	16
283	Synthesis of ZnO nanowires on steel alloy substrate by thermal evaporation: Growth mechanism and structural and optical properties. Korean Journal of Chemical Engineering, 2006, 23, 860-865.	1.2	16
284	A simulation study on the direct carbothermal reduction of SiO2 for Si metal. Current Applied Physics, 2010, 10, S218-S221.	1.1	16
285	Influence of minority charge carrier lifetime and concentration on crystalline silicon solar cells based on double antireflection coating: A simulation study. Optical Materials, 2021, 121, 111500.	1.7	16
286	Practical room temperature formaldehyde sensing based on a combination of visible-light activation and dipole modification. Journal of Materials Chemistry A, 2021, 9, 23955-23967.	5.2	16
287	Assembling Hollow Cactus-Like ZnO Nanorods with Dipole-Modified Graphene Nanosheets for Practical Room-Temperature Formaldehyde Sensing. ACS Applied Materials & Interfaces, 2022, 14, 13186-13195.	4.0	16
288	Enhanced sunlight-driven photocatalytic, supercapacitor and antibacterial applications based on graphene oxide and magnetite-graphene oxide nanocomposites. Ceramics International, 2022, 48, 29349-29358.	2.3	16

#	Article	IF	CITATIONS
289	Formation of hierarchical ZnO nanostructures "nanocombsâ€! Growth mechanism, structural and optical properties. Current Applied Physics, 2008, 8, 793-797.	1.1	15
290	A sea-cucumber-like hollow polyaniline spheres electrode-based chemical sensor for the efficient detection of aliphatic alcohols. RSC Advances, 2013, 3, 10460.	1.7	15
291	Synthesis and characterization of alkali metal molybdates with high catalytic activity for dye degradation. RSC Advances, 2016, 6, 54553-54563.	1.7	15
292	Highly stable field emission properties from well-crystalline 6-Fold symmetrical hierarchical ZnO nanostructures. Ceramics International, 2017, 43, 11753-11758.	2.3	15
293	Fabrication and Characterization of Highly Sensitive Acetone Chemical Sensor Based on ZnO Nanoballs. Materials, 2017, 10, 799.	1.3	15
294	Large-scale synthesis of coiled-like shaped carbon nanotubes using bi-metal catalyst. Applied Nanoscience (Switzerland), 2018, 8, 105-113.	1.6	15
295	<i>In Situ</i> Construction of the Coral-like Polyaniline on the Aligned Silicon Nanowire Arrays for Silicon Substrate On-chip Supercapacitors. ACS Applied Energy Materials, 2020, 3, 11792-11802.	2.5	15
296	Multi-biological combined system: A mechanistic approach for removal of multiple heavy metals. Chemosphere, 2021, 276, 130018.	4.2	15
297	Growth, Properties and Dye-Sensitized Solar Cells (DSSCs) Applications of ZnO Nanocones and Small Nanorods. Science of Advanced Materials, 2011, 3, 695-701.	0.1	15
298	Iron-Doped ZnO Nanoparticles as Potential Scaffold for Hydrazine Chemical Sensor. Sensor Letters, 2014, 12, 1273-1278.	0.4	15
299	Highly Pure Gold Nanotriangles with almost 100% Yield for Surface-Enhanced Raman Scattering. ACS Applied Nano Materials, 2022, 5, 1220-1231.	2.4	15
300	Coconut Carbon Dots: Progressive Large-Scale Synthesis, Detailed Biological Activities and Smart Sensing Aptitudes towards Tyrosine. Nanomaterials, 2022, 12, 162.	1.9	15
301	A computational study of carrier lifetime, doping concentration, and thickness of window layer for GaAs solar cell based on Al2O3 antireflection layer. Solar Energy, 2022, 234, 330-337.	2.9	15
302	Lonsdaleite diamond growth on reconstructed Si (100) by hot-filament chemical vapor deposition (HFCVD). Korean Journal of Chemical Engineering, 2003, 20, 1154-1157.	1.2	14
303	Preparation and characterization of α-FeOOH and α-Fe2O3 by sol–gel method. Journal of Materials Science, 2005, 40, 3031-3034.	1.7	14
304	Two-Step Growth of Hexagonal-Shaped ZnO Nanowires and Nanorods and Their Properties. Journal of Nanoscience and Nanotechnology, 2007, 7, 4522-4528.	0.9	14
305	ZnO Nanorod–TiO2-Nanoparticulate Electrode for Dye-Sensitized Solar Cells. Japanese Journal of Applied Physics, 2009, 48, 125003.	0.8	14
306	Effect of refluxing time on the morphology of pencil like zinc oxide nanostructures prepared by solution method. Metals and Materials International, 2010, 16, 767-772.	1.8	14

#	Article	IF	CITATIONS
307	Novel thiazolothiazole based linear chromophore for small molecule organic solar cells. Chemical Physics Letters, 2013, 574, 89-93.	1.2	14
308	Asymmetric, efficient π-conjugated organic semiconducting chromophore for bulk-heterojunction organic photovoltaics. Dyes and Pigments, 2018, 149, 141-148.	2.0	14
309	Environment-friendly and highly sensitive dichloromethane chemical sensor fabricated with ZnO nanopyramids-modified electrode. Journal of the Taiwan Institute of Chemical Engineers, 2019, 102, 143-152.	2.7	14
310	ZnO Nanocrystal-Based Chloroform Detection: Density Functional Theory (DFT) Study. Coatings, 2019, 9, 769.	1.2	14
311	Hydroxyapatite (HA) Modified Nanocoating Enhancement on AZ31 Mg Alloy by Combined Surface Mechanical Attrition Treatment and Electrochemical Deposition Approach. Journal of Nanoscience and Nanotechnology, 2019, 19, 810-818.	0.9	14
312	Exploration of fulvic acid as a functional excipient in line with the regulatory requirement. Environmental Research, 2020, 187, 109642.	3.7	14
313	New energetic indandione based planar donor for stable and efficient organic solar cells. Solar Energy, 2020, 201, 649-657.	2.9	14
314	Diode Behavior of Electrophoretically Deposited Polyaniline on TiO2 Nanoparticulate Thin Film Electrode. Journal of Nanoscience and Nanotechnology, 2011, 11, 1559-1564.	0.9	13
315	Novel liquid crystalline oligomer with thiazolothiazole-acceptor for efficient BHJ small molecule organic solar cells. Synthetic Metals, 2014, 187, 178-184.	2.1	13
316	Solution processed ZnO rectangular prism as an effective photoanode material for dye sensitized solar cells. Materials Letters, 2015, 147, 119-122.	1.3	13
317	ZnO hollow nano-baskets for mineralization of cationic dye. Materials Letters, 2016, 183, 329-333.	1.3	13
318	Manipulating the structure of polyaniline by exploiting redox chemistry: Novel p-NiO/n-polyaniline/n-Si Schottky diode based chemosensor for the electrochemical detection of hydrazinobenzene. Electrochimica Acta, 2016, 215, 200-211.	2.6	13
319	Effective and stable FeNi@ N-doped graphene counter electrode for enhanced performance dye sensitized solar cells. Materials Letters, 2017, 191, 80-84.	1.3	13
320	Spiro-bifluorene core based hole transporting material with graphene oxide modified CH3NH3PbI3 for inverted planar heterojunction solar cells. Electrochimica Acta, 2019, 319, 885-894.	2.6	13
321	Solution processed bulk heterojunction organic solar cells using small organic semiconducting materials based on fluorene core unit. Optical Materials, 2019, 91, 425-432.	1.7	13
322	β-AgVO3 nanowires/TiO2 nanoparticles heterojunction assembly with improved visible light driven photocatalytic decomposition of hazardous pollutants and mechanism insight. Separation and Purification Technology, 2020, 251, 117271.	3.9	13
323	Distinctive polypyrrole nanobelts as prospective electrode for the direct detection of aliphatic alcohols: Electrocatalytic properties. Applied Catalysis B: Environmental, 2014, 144, 665-673.	10.8	12
324	Controlled growth of single-crystalline nanostructured dendrites of α-Fe2O3 blended with MWCNT: a systematic investigation of highly selective determination of l-dopa. RSC Advances, 2014, 4, 23050.	1.7	12

#	Article	IF	CITATIONS
325	Spindles shaped ZnO modified glassy carbon electrode for the selective monitoring of piperidine. Materials Letters, 2015, 148, 188-191.	1.3	12
326	Influence of annealing treatment on phase transformation of Ga15Se77Tl8 thin films. Journal of Materials Science: Materials in Electronics, 2016, 27, 8227-8233.	1.1	12
327	Ag-doped ZnO nanoellipsoids based highly sensitive gas sensor. Materials Express, 2017, 7, 380-388.	0.2	12
328	Direct Growth of Flower-Shaped ZnO Nanostructures on FTO Substrate for Dye-Sensitized Solar Cells. Crystals, 2019, 9, 405.	1.0	12
329	Ytterbium-Doped ZnO Flowers Based Phenyl Hydrazine Chemical Sensor. Journal of Nanoscience and Nanotechnology, 2019, 19, 4199-4204.	0.9	12
330	Enticing 3D peony-like ZnGa2O4 microstructures for electrochemical detection of N, N-dimethylmethanamide chemical. Journal of Hazardous Materials, 2021, 404, 124069.	6.5	12
331	Influence of gamma-irradiation on the optical and structural properties of Se85Te15-xBix nano-thin chalcogenide films. Radiation Physics and Chemistry, 2021, 188, 109659.	1.4	12
332	A Facile Synthesis of ZnO Nanoparticles and Its Application as Photoanode for Dye Sensitized Solar Cells. Science of Advanced Materials, 2015, 7, 1137-1142.	0.1	12
333	CarbonIron Electron Transport Channels in Porphyrin–Graphene Complex for ppb‣evel Room Temperature NO Gas Sensing. Small, 2022, 18, e2103259.	5.2	12
334	Electrical and Structural Characterization of Plasma Polymerized Polyaniline/TiO <sub>2</sub> Heterostructure Diode: A Comparative Study of Single and Bilayer TiO <sub>2</sub> Thin Film Electrode. Journal of Nanoscience and Nanotechnology, 2011, 11, 3306-3313.	0.9	11
335	Ti thin film towards the growth of crystalline-TiO2 nanostructures: stepped light-induced transient measurements of photocurrent and photovoltage in dye sensitized solar cell. CrystEngComm, 2014, 16, 3020.	1.3	11
336	Ni–Co bimetallic nanoparticles anchored reduced graphene oxide as an efficient counter electrode for the application of dye sensitized solar cells. Journal of Materials Science: Materials in Electronics, 2017, 28, 823-831.	1.1	11
337	In vitro microcosm of co-cultured bacteria for the removal of hexavalent Cr and tannic acid: A mechanistic approach to study the impact of operational parameters. Ecotoxicology and Environmental Safety, 2021, 208, 111484.	2.9	11
338	Tetracyanonickelate (II)/KOH/reduced graphene oxide fabricated carbon felt for mediated electron transfer type electrochemical sensor for efficient detection of N2O gas at room temperature. Environmental Research, 2021, 201, 111591.	3.7	11
339	Refined optoelectronic properties of silicon nanowires for improving photovoltaic properties of crystalline solar cells: a simulation study. Journal of Materials Science: Materials in Electronics, 2021, 32, 2784-2795.	1.1	11
340	Indandione oligomer@graphene oxide functionalized nanocomposites for enhanced and selective detection of trace Cr2+ and Cu2+ ions. Advanced Composites and Hybrid Materials, 2022, 5, 1582-1594.	9.9	11
341	Sensitivity enhancement of SPR biosensor employing heterostructure blue phosphorus/MoS <sub>2</sub> and silicon layer. Emerging Materials Research, 2022, 11, 239-250.	0.4	11
342	Growth of ZnO nanoneedles on silicon substrate by cyclic feeding chemical vapor deposition: Structural and optical properties. Korean Journal of Chemical Engineering, 2007, 24, 1084-1088.	1.2	10

#	Article	IF	CITATIONS
343	High Aspect-Ratio ZnO Nanowires Based Nanoscale Field Effect Transistors. Journal of Nanoscience and Nanotechnology, 2009, 9, 2692-2697.	0.9	10
344	Effect of electron beam irradiation on the electrochemical properties of heteropolyacid–polyethylene oxide composite electrolyte for dye-sensitized solar cell. Current Applied Physics, 2010, 10, S161-S164.	1.1	10
345	Optical Analysis of Zinc Oxide Quantum Dots with Bovine Serum Albumin and Bovine Hemoglobin. Journal of Pharmaceutical Innovation, 2014, 9, 48-52.	1.1	10
346	Quantitative determination of raw and functionalized carbon nanotubes for the antibacterial studies. Journal of Materials Science, 2014, 49, 4288-4296.	1.7	10
347	Ethylene-VInyl acetate/LDH nanocomposites with enhanced thermal stability, flame retardancy, and rheological property. Polymer Composites, 2016, 37, 3449-3459.	2.3	10
348	A novel perovskite solar cell design using aligned TiO <sub>2</sub> nano-bundles grown on a sputtered Ti layer and a benzothiadiazole-based, dopant-free hole-transporting material. Nanoscale, 2017, 9, 17544-17550.	2.8	10
349	Synthesis, Characterization, Photocatalytic and Sensing Properties of Mn-Doped ZnO Nanoparticles. Journal of Nanoscience and Nanotechnology, 2019, 19, 8095-8103.	0.9	10
350	Influence of Donor Groups on Benzoselenadiazole-Based Dopant-Free Hole Transporting Materials for High Performance Perovskite Solar Cells. ACS Applied Energy Materials, 2021, 4, 312-321.	2.5	10
351	Hydrogen Storage Properties of Heterostructured Zinc Oxide Nanostructures. Journal of Nanoengineering and Nanomanufacturing, 2011, 1, 188-195.	0.3	10
352	Effect of Nickel Doping on the Properties of Hydroxyapatite Nanoparticles. Journal of Nanoscience and Nanotechnology, 2020, 20, 2482-2487.	0.9	10
353	Iron Oxide Nanocubes for Photocatalytic Degradation and Antimicrobial Applications. Nanoscience and Nanotechnology Letters, 2016, 8, 1014-1019.	0.4	10
354	Seed germination studies on Chickpeas, Barley, Mung beans and Wheat with natural biomass and plastic waste derived C-dots. Science of the Total Environment, 2022, 837, 155593.	3.9	10
355	HFCVD grown graphene like carbon–nickel nanocomposite thin film as effective counter electrode for dye sensitized solar cells. Materials Research Bulletin, 2013, 48, 4538-4543.	2.7	9
356	Insight into calcification of Synechocystis sp. enhanced by extracellular carbonic anhydrase. RSC Advances, 2016, 6, 29811-29817.	1.7	9
357	Beckmann Rearrangement of Cyclohexanone Oxime Using Nanocrystalline Titanium Silicalite-1 (TS-1). Journal of Nanoscience and Nanotechnology, 2017, 17, 2170-2176.	0.9	9
358	Electrical properties of Ga-doped ZnO nanowires/Si heterojunction diode. Materials Express, 2020, 10, 794-801.	0.2	9
359	An insight into the mechanism of â€~symbiotic-bioremoval' of heavy metal ions from synthetic and industrial samples using bacterial consortium. Environmental Technology and Innovation, 2021, 21, 101302.	3.0	9
360	Charge transfer driven by redox dye molecules on graphene nanosheets for room-temperature gas sensing. Nanoscale, 2021, 13, 18596-18607.	2.8	9

#	Article	IF	CITATIONS
361	Low-temperature synthesis of cadmium-doped zinc oxide nanosheets for enhanced sensing and environmental remediation applications. Journal of Alloys and Compounds, 2021, 863, 158649.	2.8	9
362	Selective ethanol gas sensing performance of flower-shaped CuO composed of thin nanoplates. Journal of Materials Science: Materials in Electronics, 2021, 32, 18565-18579.	1.1	9
363	Highly Sensitive and Selective Eco-Toxic 4-Nitrophenol Chemical Sensor Based on Ag-Doped ZnO Nanoflowers Decorated with Nanosheets. Molecules, 2021, 26, 4619.	1.7	9
364	Development of Ethanol Gas Sensor Using α-Fe2O3 Nanocubes Synthesized by Hydrothermal Process. Journal of Nanoelectronics and Optoelectronics, 2020, 15, 59-64.	0.1	9
365	Refluxing Synthesis of Anatase TiO <sub>2</sub> Nanoparticles Assembled Microprisms and Its Application for Dye-Sensitized Solar Cells. Science of Advanced Materials, 2014, 6, 459-464.	0.1	9
366	An In-Depth Optimization of Thickness of Base and Emitter of ZnO/Si Heterojunction-Based Crystalline Silicon Solar Cell: A Simulation Method. Journal of Electronic Materials, 2022, 51, 586-593.	1.0	9
367	Study on the structural and optical properties of Cd1â^'x Zn x O layers enhanced by rapid thermal annealing. Electronic Materials Letters, 2011, 7, 215-220.	1.0	8
368	A study on photo-induced crystallization in Ga10Se78Tl12 thin films. Journal of Materials Science: Materials in Electronics, 2015, 26, 6206-6211.	1.1	8
369	High sensitivity Schottky junction diode based on monolithically grown aligned polypyrrole nanofibers: Broad range detection of m-dihydroxybenzene. Analytica Chimica Acta, 2015, 886, 165-174.	2.6	8
370	Efficient spirobifluorene-core electron-donor material for application in solution-processed organic solar cells. Chemical Physics Letters, 2016, 663, 137-144.	1.2	8
371	Ytterbium Doped Zinc Oxide Nanopencils for Chemical Sensor Application. Journal of Nanoscience and Nanotechnology, 2017, 17, 9157-9162.	0.9	8
372	Multiscale Interface Effect on Homogeneous Dielectric Structure of ZrO2/Teflon Nanocomposite for Electrowetting Application. Polymers, 2018, 10, 1119.	2.0	8
373	Charge-Transporting Materials for Perovskite Solar Cells. Advances in Inorganic Chemistry, 2018, , 185-246.	0.4	8
374	Frictional Reduction with Partially Exfoliated Multi-Walled Carbon Nanotubes as Water-Based Lubricant Additives. Journal of Nanoscience and Nanotechnology, 2018, 18, 3427-3432.	0.9	8
375	Furosemide–Cetyltrimethylammonium Bromide Interactions in Aqueous Dimethylsulfoxide Solutions: Physico–Chemical Studies. Zeitschrift Fur Physikalische Chemie, 2019, 233, 413-430.	1.4	8
376	Iron Oxide Nanoparticles as Potential Scaffold for Photocatalytic and Sensing Applications. Journal of Nanoscience and Nanotechnology, 2019, 19, 2695-2701.	0.9	8
377	Investigation of newly designed asymmetric chromophore in view of power conversion efficiency improvements for organic solar cells. Materials Letters, 2020, 260, 126865.	1.3	8
378	Effective photocatalytic dye degradation using low temperature grown zinc oxide nanostructures. Materials Letters, 2020, 281, 128609.	1.3	8

#	Article	IF	CITATIONS
379	Development and Characterization of Solar Simulator for Solar Cells. Journal of Nanoelectronics and Optoelectronics, 2020, 15, 720-724.	0.1	8
380	Synthesis of Sn-Doped ZnO Nanostructures for 4-Nitrophenol Chemical Sensor Application. Nanoscience and Nanotechnology Letters, 2016, 8, 827-832.	0.4	8
381	Growth and Properties of Sn-Doped ZnO Nanowires for Heterojunction Diode Application. Science of Advanced Materials, 2014, 6, 1993-2000.	0.1	8
382	Polyaniline-Functionalized TiO <sub>2</sub> Nanoparticles as a Suitable Matrix for Hydroquinone Sensor. Science of Advanced Materials, 2017, 9, 2032-2038.	0.1	8
383	Determinantal study on the thickness of graphene oxide as ARC layer for silicon solar cells using: A simulation approach. Materials Science in Semiconductor Processing, 2022, 147, 106695.	1.9	8
384	Diamond nucleation enhancement on reconstructed Si(100). Journal of Vacuum Science and Technology A: Vacuum, Surfaces and Films, 2002, 20, 202-205.	0.9	7
385	Effect of Electron Beam Irradiation on the Properties of Polyethylene Oxide–TiO <sub>2</sub> Composite Electrolyte for Dye Sensitized Solar Cells. Materials Science Forum, 0, 658, 161-164.	0.3	7
386	Direct Growth of ZnO Nanosheets on FTO Substrate for Dye-Sensitized Solar Cells Applications. Journal of Nanoscience and Nanotechnology, 2010, 10, 6666-6671.	0.9	7
387	Studies on phase change Ge15Se77Sb8 thin films by laser irradiation. Journal of Materials Science: Materials in Electronics, 2016, 27, 2426-2429.	1.1	7
388	Nanoprecursor-Mediated Synthesis of Mg <sup>2+</sup> -Doped TiO <sub>2</sub> Nanoparticles and Their Application for Dye-Sensitized Solar Cells. Journal of Nanoscience and Nanotechnology, 2016, 16, 744-752.	0.9	7
389	Preparation and Characterization of Highly Efficient CuFe Mixed Oxides for Total Oxidation of Toluene. Journal of Nanoscience and Nanotechnology, 2018, 18, 3381-3386.	0.9	7
390	Highly Sensitive Picric Acid Chemical Sensor Based on Samarium (Sm) Doped ZnO Nanorods. Journal of Nanoscience and Nanotechnology, 2019, 19, 3637-3642.	0.9	7
391	Surface Modification of Bentonite with Polymer Brushes and Its Application as an Efficient Adsorbent for the Removal of Hazardous Dye Orange I. Nanomaterials, 2020, 10, 1112.	1.9	7
392	Underlying effects of diiodooctane as additive on the performance of bulk heterojunction organic solar cells based small organic molecule of isatin-core moiety. Synthetic Metals, 2020, 261, 116304.	2.1	7
393	α-MnO2 Nanowires as Potential Scaffolds for a High-Performance Formaldehyde Gas Sensor Device. Coatings, 2021, 11, 860.	1.2	7
394	Low-Temperature Growth of Flower-Shaped UV-Emitting ZnO Nanostructures on Steel Alloy by Thermal Evaporation. Journal of Nanoscience and Nanotechnology, 2007, 7, 4421-4427.	0.9	6
395	Composite electrolytes of polyethylene glycol methyl ether and TiO2 for dye-sensitized solar cells—Effect of heat treatment. Materials Chemistry and Physics, 2011, 127, 479-483.	2.0	6
396	Electric-field induced layer-by-layer assembly technique with single component for construction of conjugated polymer films. RSC Advances, 2015, 5, 58499-58503.	1.7	6

#	Article	IF	CITATIONS
397	Towards design of metal oxide free perovskite solar cell paradigm: Materials processing and enhanced device performance. Chemical Engineering Journal, 2015, 281, 599-605.	6.6	6
398	Fabrication and Characterizations of Ethanol Sensor Based on CuO Nanoparticles. Journal of Nanoscience and Nanotechnology, 2018, 18, 2892-2897.	0.9	6
399	Biosynthesis, Characterization and Biological Activities of Silver Nanoparticles from <i>Pogostemon cablin</i> Benth. Methanolic Leaf Extract. Journal of Nanoscience and Nanotechnology, 2019, 19, 4109-4115.	0.9	6
400	Methylene blue intercalated layered MnO2 nanosheets for high-sensitive non-enzymatic ascorbic acid sensor. Journal of Materials Science: Materials in Electronics, 2021, 32, 8317-8329.	1.1	6
401	An exploration of 3-methoxypropionitrile chemical sensor based on layered hexagonal NiCo2O4 nanoplates as electrode material. Ceramics International, 2021, 47, 15357-15366.	2.3	6
402	The co-modification of MoS2 and CdS on TiO2 nanotube array for improved photoelectrochemical properties. Ionics, 2021, 27, 4371-4381.	1.2	6
403	p-CuO/n-ZnO Heterojunction Structure for the Selective Detection of Hydrogen Sulphide and Sulphur Dioxide Gases: A Theoretical Approach. Coatings, 2021, 11, 1200.	1.2	6
404	Electrical Sensor Based on Hollow ZnO Spheres for Hydrazine Detection. Journal of Nanoelectronics and Optoelectronics, 2018, 13, 1769-1776.	0.1	6
405	Semiconducting Nanostructures and Nanocomposites for the Recognition of Toxic Chemicals (A) Tj ETQq1	1 0.784314 rg₿⊺ 0.1	Г ¦Overlock
406	ZnO-nanowire-covered TiO\$_{2} Thin-film Electrodes for Improvingthe Photovoltaic Properties of Dye-sensitized Solar Cells. Journal of the Korean Physical Society, 2009, 55, 89-93.	0.3	6
407	Three-Dimensional Graphene-Based Foams with "Greater Electron Transferring Areas―Deriving High Gas Sensitivity. ACS Applied Nano Materials, 2021, 4, 13234-13245.	2.4	6
408	Approaching high performance Ni(Co) molybdate electrode materials for flexible hybrid devices. RSC Advances, 2022, 12, 14858-14864.	1.7	6
409	Growth of Yttria tabilized Zirconia Thin Films on Textured Silver Substrates by Chemical Vapor Deposition. Journal of the American Ceramic Society, 2002, 85, 1897-1899.	1.9	5
410	Effect of tungsten/filament on the growth of carbon nanotubes in hot filament chemical vapor deposition system. Journal of Materials Science, 2004, 39, 5771-5777.	1.7	5
411	Magnesium interlayered diamond coating on silicon. International Journal of Refractory Metals and Hard Materials, 2006, 24, 418-426.	1.7	5
412	Functionalized vertical GaN micro pillar arrays with high signal-to-background ratio for detection and analysis of proteins secreted from breast tumor cells. Scientific Reports, 2017, 7, 14917.	1.6	5
413	Smoke sensing applications of Brij 58 functionalized Praseodymium oxide (Pr6O11) nanostructures. Sensors and Actuators B: Chemical, 2019, 297, 126628.	4.0	5
414	Enhanced Photocatalytic Performance of Sn <sub>6</sub> SiO <sub>8</sub> Nanoparticles and Their Reduced Graphene Oxide (rGO) Nanocomposite. Journal of Nanoscience and Nanotechnology, 2020, 20, 5426-5432.	0.9	5

#	Article	IF	CITATIONS
415	Planar D-ï€-A Configured Dimethoxy Vinylbenzene Based Small Organic Molecule for Solution-Processed Bulk Heterojunction Organic Solar Cells. Applied Sciences (Switzerland), 2020, 10, 5743.	1.3	5
416	In Vitro Bioadsorption of Cd2+ Ions: Adsorption Isotherms, Mechanism, and an Insight to Mycoremediation. Processes, 2020, 8, 1085.	1.3	5
417	Benzoselenadiazoleâ€core asymmetric Dâ€Aâ€A small molecule for solution processed bulk heterojunction organic solar cells. International Journal of Energy Research, 2020, 44, 12100-12111.	2.2	5
418	Synthesis and electrochemical properties of Ge4+ ions-modified VO2(paramontroseite). Journal of Materials Science: Materials in Electronics, 2020, 31, 3795-3802.	1.1	5
419	Ultrathin Leaf-Shaped CuO Nanosheets Based Sensor Device for Enhanced Hydrogen Sulfide Gas Sensing Application. Chemosensors, 2021, 9, 221.	1.8	5
420	Synthesis of Iron Oxide@Pt Core–Shell Nanoparticles for Reductive Conversion of Cr(VI) to Cr(III) and Antibacterial Studies. Journal of Nanoscience and Nanotechnology, 2020, 20, 918-923.	0.9	5
421	ZnO Balls Made of Intermingled Nanocrystalline Nanosheets for Photovoltaic Device Application. Science of Advanced Materials, 2014, 6, 562-568.	0.1	5
422	Realizing high performance flexible supercapacitors by electrode modification. RSC Advances, 2021, 11, 39045-39050.	1.7	5
423	Highly stable bulk heterojunction organic solar cells based on asymmetric benzoselenadiazoleâ€oriented organic chromophores. International Journal of Energy Research, 2022, 46, 7825-7839.	2.2	5
424	Crystalline structure of YSZ thin films deposited on Si(111) substrate by chemical vapor deposition. Korean Journal of Chemical Engineering, 1998, 15, 243-245.	1.2	4
425	Preparation of superconducting Y-Ba-Cu-O films by aerosol assisted chemical vapor deposition using liquid solution sources. Korean Journal of Chemical Engineering, 2000, 17, 524-527.	1.2	4
426	Effect of MgO interlayer on diamond film growth on silicon (100). Thin Solid Films, 2006, 497, 103-108.	0.8	4
427	Thermally Grown ZnO Nanosheets for High Efficiency Dye-Sensitized Solar Cells. Journal of Nanoscience and Nanotechnology, 2010, 10, 3654-3658.	0.9	4
428	Probe Into the Influence of Crosslinking on CO2 Permeation of Membranes. Scientific Reports, 2017, 7, 40082.	1.6	4
429	CePdâ€Nanoparticlesâ€Incorporated Carbon Nanofibers as Efficient Counter Electrode for DSSCs. ChemistrySelect, 2018, 3, 12314-12319.	0.7	4
430	Protein (bovine serum albumin) driven copper selenide and copper telluride nanostructures: structural, optical and electrical properties. Journal of Materials Science: Materials in Electronics, 2019, 30, 11317-11326.	1.1	4
431	Justifying benzoselenadiazole acceptor core as organic semiconductor for stable bulk-heterojunction organic solar cells at ambient temperature. Journal of Materiomics, 2021, 7, 1112-1121.	2.8	4
432	Perforated ZnO Nanotube/TiO2 Thin Film Electrode-Based Dye Sensitized Solar Cells. Journal of the Korean Physical Society, 2010, 56, 813-817.	0.3	4

#	Article	IF	CITATIONS
433	Aluminum Doped ZnO Nanorods for Enhanced Phenylhydrazine Chemical Sensor Applications. Science of Advanced Materials, 2021, 13, 2483-2488.	0.1	4
434	Cauliflower-Shaped ZnO Nanostructure for Enhanced NO <sub>2</sub> Gas Sensor Application. Science of Advanced Materials, 2021, 13, 2358-2363.	0.1	4
435	Sustainable agronomic response of carbon quantum dots on Allium sativum: Translocation, physiological responses and alternations in chromosomal aberrations. Environmental Research, 2022, 212, 113559.	3.7	4
436	High-Yield Synthesis and Properties of Symmetrical Comb-Like ZnO Nanostructures on Aluminum Foil Substrate. Journal of Nanoscience and Nanotechnology, 2010, 10, 2381-2388.	0.9	3
437	Growth of Aligned Hexagonal ZnO Nanorods on FTO Substrate for Dye-Sensitized Solar Cells (DSSCs) Application. Journal of Nanoscience and Nanotechnology, 2011, 11, 3560-3564.	0.9	3
438	Bifunction-Integrated Dielectric Nanolayers of Fluoropolymers with Electrowetting Effects. Materials, 2018, 11, 2474.	1.3	3
439	Influence of Incorporated Barium Ion on the Physio-Chemical Properties of Zinc Oxide Nanodisks Synthesized via a Sonochemical Process. Journal of Nanoscience and Nanotechnology, 2020, 20, 5452-5457.	0.9	3
440	Structural, Optical and Magnetic Properties of Zn <sub>1-<i>x</i></sub> Co <sub><i>x</i></sub> O Nanoparticles. Journal of Nanoscience and Nanotechnology, 2020, 20, 5525-5532.	0.9	3
441	Controlled Growth of WO3 Pyramidal Thin Film via Hot-Filament Chemical Vapor Deposition: Electrochemical Detection of Ethylenediamine. Chemosensors, 2021, 9, 257.	1.8	3
442	Nanocrystalline ZnO Flakes for Photovoltaic Device Applications. Advanced Science Letters, 2010, 3, 543-547.	0.2	3
443	Influence of CeO2 nanoparticles synthesized from plant extracts on the catalytic performance of isolated catalase from carrots. Emergent Materials, 2022, 5, 673-682.	3.2	3
444	Corrosion behavior of high-temperature superconductor YBa2Cu3-yAgyO7-x in the presence of water. Korean Journal of Chemical Engineering, 1995, 12, 563-566.	1.2	2
445	Effect of deposition temperature on the growth of Y1Ba2Cu3O7â <sup>~</sup> 'x thin film by aerosol assisted chemical vapor deposition using liquid solution sources. Korean Journal of Chemical Engineering, 2003, 20, 772-775.	1.2	2
446	Influence of the silicon surface treatment by plasma etching and scratching on the nucleation of diamond grown in HFCVD - a comparative study. Korean Journal of Chemical Engineering, 2008, 25, 593-598.	1.2	2
447	New and effective anti reflection coating of SiC-SiO2 nanocomposite for p-type silicon solar cell. , 2015, , .		2
448	Effect of TiO2 Particle Size on the Performance of Flexible Dye Sensitized Solar Cells. Journal of Nanoscience and Nanotechnology, 2015, 15, 6675-6679.	0.9	2
449	Hydrodechlorination of Silicon Tetrachloride to Trichlorosilane Over Ordered Mesoporous Carbon Catalysts: Effect of Pretreatment of Oxygen and Hydrochloric Acid. Journal of Nanoscience and Nanotechnology, 2016, 16, 1802-1805.	0.9	2
450	Fabrication and Characterization of Dye-Sensitized Solar Cells Based on Flower Shaped ZnO Nanostructures. Journal of Nanoscience and Nanotechnology, 2018, 18, 3697-3701.	0.9	2

#	Article	IF	CITATIONS
451	Introductory Chapter: An Introduction to Nanoporous Materials. , 0, , .		2
452	Ni-Doped ZnO Thin Films: Deposition, Characterization and Photocatalytic Applications. Journal of Nanoscience and Nanotechnology, 2021, 21, 1560-1569.	0.9	2
453	MnO2 Nanoparticles Anchored Multi Walled Carbon Nanotubes as Potential Anode Materials for Lithium Ion Batteries. Journal of Nanoscience and Nanotechnology, 2021, 21, 5296-5301.	0.9	2
454	An Effective D-Ï€-A Type Donor Material Based on 4-Fluorobenzoylacetonitrile Core Unit for Bulk Heterojunction Organic Solar Cells. Applied Sciences (Switzerland), 2021, 11, 646.	1.3	2
455	Plasma Deposited Polyaniline on Ruthenium Dye Sensitized Zno Thin Film for Dye Sensitized Solar Cell. Advanced Science Letters, 2012, 18, 132-136.	0.2	2
456	Hetero-aggregation behaviour of green copper nanoparticles: Course interactions with environmental components. Separation and Purification Technology, 2022, 284, 120177.	3.9	2
457	Nanocomposite (S <sub>3</sub> Sb <sub>2</sub> ) <sub> <i>x</i> </sub> (S <sub>2</sub> Ge) <sub>100â^'<i>x</i> </sub> chalcogenide glasses: structural and physical properties. Emerging Materials Research, 2022, 11, 185-192.	0.4	2
458	Highly Sensitive and Selective Sulfite Ion Sensor Based on Biochemically Stable Iodoâ€Functionalized Coumarin Fluorophores. ChemistrySelect, 2022, 7, .	0.7	2
459	Characteristics of Y1Ba2Cu3O7-x high-T c superconductor prepared by partial melting process. Korean Journal of Chemical Engineering, 1998, 15, 304-309.	1.2	1
460	Quasi-Solid State Dye Sensitized Solar Cell Based on Poly (Acrylonitrile-co-Methacrylonitrile)-Silica Gel Electrolyte. , 2006, , .		1
461	Effective inorganic-organic composite electrolytes for efficient solid-state dye sensitized solar cells. , 2013, , .		1
462	Effects of cobalt and cobalt oxide buffer layers on nucleation and growth of hot filament chemical vapor deposition diamond films on silicon (100). Korean Journal of Chemical Engineering, 2014, 31, 1271-1275.	1.2	1
463	Optimized Ultrasharp Silicon Nanowire Geometries for Enhanced Field Ionization Properties. Materials Research Society Symposia Proceedings, 2015, 1785, 7-11.	0.1	1
464	Flower-Shaped Mg <sub>3</sub> Al <sub>1â^'<i>x</i></sub> Fe <sub><i>x</i></sub> –CO <sub>3</sub> Layered Double Hydroxides Derived Adsorbents with Tunable Memory Effect for Environmental Remediation. Journal of Nanoscience and Nanotechnology, 2018, 18, 2609-2615.	0.9	1
465	High Aspect Ratio Perforated Co3O4 Nanowires Derived from Cobalt-Carbonate-Hydroxide Nanowires with Enhanced Sensing Performance. Journal of Nanoscience and Nanotechnology, 2018, 18, 3499-3504.	0.9	1
466	Electrochemical Detection of Chloride Ions by Copper (II) Complex with Mixed Ligand of Oxindole Derivative and Dithiocarbamates Moiety. Applied Sciences (Switzerland), 2019, 9, 1358.	1.3	1
467	Visible-Light Driven Effective Photocatalytic Degradation of Methylene Blue Dye Using Perforated Curly Zn <sub>0.1</sub> Ni <sub>0.9</sub> O Nanosheets. Journal of Nanoscience and Nanotechnology, 2020, 20, 5759-5764.	0.9	1
468	Electrochemical behavior of uniformly decorated electrospun nickel on carbon nanofibers. Molecular Catalysis, 2021, 504, 111458.	1.0	1

#	Article	lF	CITATIONS
469	Effective Metal Loaded Polyaniline Nanofibers Based Potent Counter Electrode for Solar Energy Conversion. Science of Advanced Materials, 2013, 5, 21-27.	0.1	1
470	Synthesis of BaTiO <sub>3</sub> and SrTiO <sub>3</sub> Nanoparticles: Effect of Annealing Temperatures on Their Morphological, Crystalline, Optical and Photovoltaic Properties. Nanoscience and Nanotechnology Letters, 2016, 8, 896-902.	0.4	1
471	Co-Doped ZnO Nano-Agglomerates as a Potential Scaffold for Non-Enzymatic Hydrogen Peroxide Sensing. Science of Advanced Materials, 2021, 13, 1732-1738.	0.1	1
472	Analysing biosensor clinical pathogen information using mayfly optimized convolute neural network approach. Expert Systems, 0, , .	2.9	1
473	Metal-Organic Framework Fabricated V2O5 Cathode Material for High-Performance Lithium-Ion Batteries. Coatings, 2022, 12, 844.	1.2	1
474	Controllable Synthesis of ZnO Nanonails by Vapor-Solid Process: Growth Mechanism and Structural and Optical Properties. Materials Research Society Symposia Proceedings, 2006, 957, 1.	0.1	0
475	A Solution Method for Large-scale Selective Growth of Aligned ZnO Nanorods. Materials Research Society Symposia Proceedings, 2006, 957, 1.	0.1	0
476	A novel composite electrolyte of titania nanotubes as fillers and polyethylene gycol for dye-sensitized solar cells. , 2009, , .		0
477	Growth and Properties of Ultra-Violet Emitting Aligned Zinc Oxide Nanocones with Hexagonal Caps. Journal of Nanoscience and Nanotechnology, 2010, 10, 6659-6665.	0.9	0
478	Composite of carbon nanomaterials and polyethylene oxide for dye sensitized solar cells. , 2011, , .		0
479	Graphene thin film based counter electrode for dye-sensitized solar cell. , 2011, , .		0
480	An Introduction to Graphene Materials. , 0, , .		0
481	Development of Solar/Thermal Energy Hybrid Furnace and Its Evaluation for Magnesium Extraction. Journal of Nanoelectronics and Optoelectronics, 2017, 12, 711-716.	0.1	0
482	The Synergetic Effect of MoSO <sub>2</sub> /Graphite Nanosheets as Highly Efficient for Electrochemical Water Splitting in Acidic Media. Science of Advanced Materials, 2021, 13, 1574-1583.	0.1	0
483	Interstitial Bimetallic Doping into Carbon Nanofibers By Electrospinning Technique: Electrochemical Supercapacitors. ECS Meeting Abstracts, 2020, MA2020-02, 581-581.	0.0	0
484	Investigation of Anions Effects on the Morphology of NiO Nanostructures and Their Non-Enzymatic Glucose Sensing Applications. Science of Advanced Materials, 2021, 13, 1739-1747.	0.1	0
485	Hierarchical ZnO nanostructures: growth and optical properties. Journal of Nanoscience and Nanotechnology, 2008, 8, 6355-60.	0.9	0
486	Responsive Policy Decisions for Improving the Accuracy of Medical Data Analysis in Healthcare based Human Machine Interaction Systems. International Journal of Humanoid Robotics, 0, , .	0.6	0

#	Article	IF	CITATIONS
487	The coupled electrocatalyst synergy fabrication for the electrochemical oxygen evolution reaction: From electrode to green energy system. Journal of the Chinese Chemical Society, 0, , .	0.8	0